Advances in Computational Design, *Vol. 6, No. 2 (2021) 117-133*
DOI: https://doi.org/10.12989/acd.2021.6.2.117

Modeling and analysis of the imperfect FGM-damaged RC hybrid beams

Rabahi Abderezak, Tahar Hassaine Daouadji* and Benferhat Rabia

Laboratory of Geomatics and Sustainable Development, University of Tiaret, Algeria

(Received March 27, 2020, Revised July 18, 2020, Accepted January 4, 2021)

Abstract. The use of externally bonded composite materials for strengthening reinforced concrete structures has received considerable attention in recent years. Since, concrete is a relatively fragile material and will fail when subject to the influence of many factors whose origins can be mechanical, physicochemical and accidental or related to the design and miscalculations. The bonding of FRP plate to reinforced concrete structure, appeared in the middle of the fourtwenties years, proves to be a promising and fully justified technique. In this paper, an analysis and modeling of the concentrations of interfacial stresses in a damaged reinforced concrete beam strengthening in bending by an imperfect FGM plate, was presented, based on a development of a mathematical formulation taking into account the theory of beams. The theoretical predictions are compared with other existing solutions. This research is helpful for the understanding on mechanical behaviour of the interface and design of the imperfect FGM – damaged RC hybrid structures.

Keywords: interfacial stresses; damaged RC beam; strengthening; imperfect FGM plate

1. Introduction

A concrete civil engineering structure is sized for an average life of one hundred years. However, several types of disorders reduce this forecast lifespan and today, one in three structures requires maintenance to ensure the safety of users. Numerous repairs and structural pathologies resulting from design errors during sizing or during execution, defects in resistance to shearing or bending due to excessive loading, as well as that linked to the fatigue of the structure under various loadings are at the origin of the reduction of the theoretical lifespan of a structure. In the light of these results, new directions concerning construction techniques have prompted us to think about on new rehabilitation methods in order to remedy these problems.

At present, the needs in terms of maintenance, repair and rehabilitation of civil engineering works are therefore very important than their dimensioning or their realization since they directly condition their durability. Faced with this problem, repair or reinforcement by bonding of composite materials turns out to be a promising technique. Nowadays, the reinforcement technique by external bonding of composite is one of the most used rehabilitation methods; and can contribute to the rapid and effective repair of structures, as it can also restore to the load-bearing

*Corresponding author, Ph.D. Professor, E-mail: daouadjitahar@gmail.com

http://www.techno-press.org/?journal=acd&subpage=7 ISSN: 2383-8477 (Print), 2466-0523 (Online)

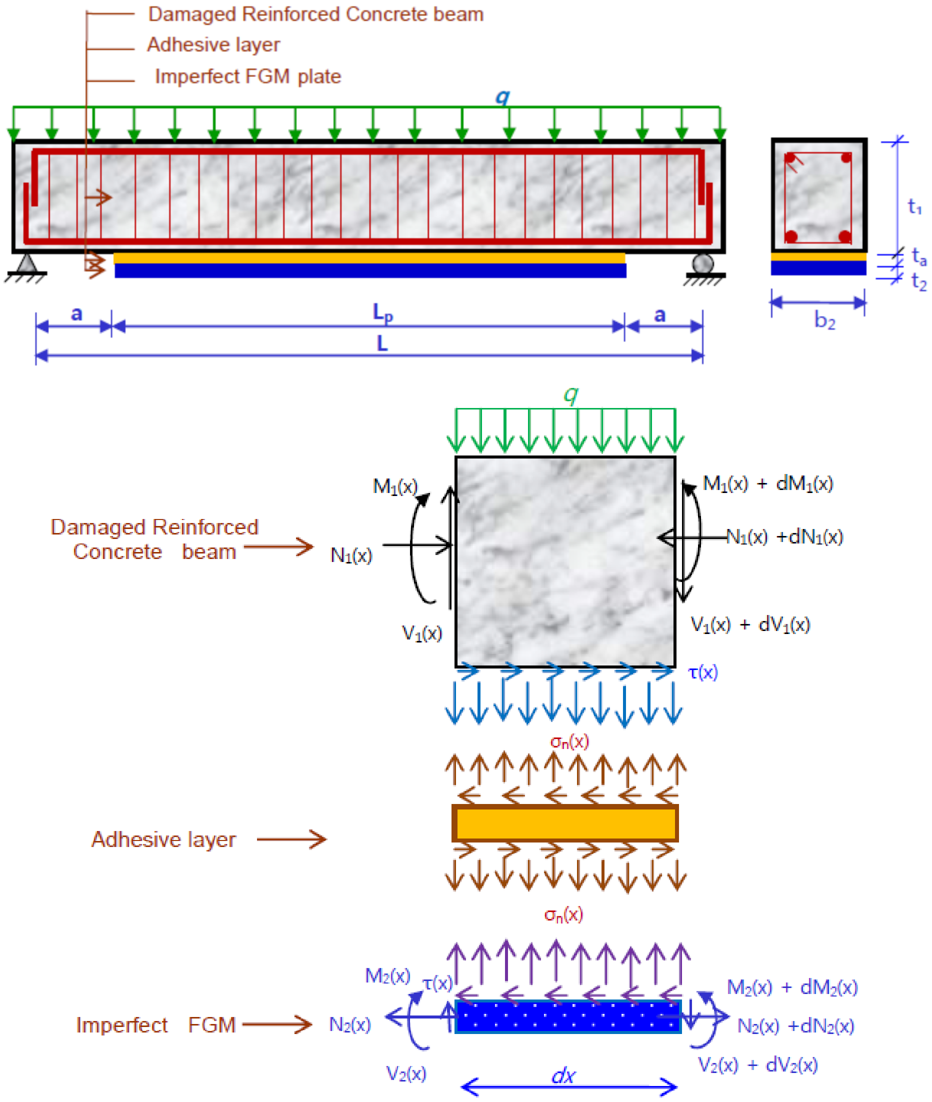

Fig 1. Simply supported damaged reinforced concrete beam strengthened bonded with porous FGM plate

elements their resistance, their rigidity and their bearing capacity. However, an important problem associated with the reinforcement in bending of reinforced concrete beams by composite materials is the peeling off of the strengthening composite plate (Smith *et al*.Teng 2002, Tounsi 2006, Hassaine Daouadji *et al*. 2016b, Bensattalah *et al*. 2018, Chergui *et al*. 2019, Chaded *et al*. 2018, Hadji *et al*. 2015, Hamrat *et al*. 2020, Hassaine Daouadji *et al*. 2020, Abdelhak *et al*. 2016, Abdedezak *et al*. 2018, Benhenni *et al*. 2018, Rabahi *et al*. 2020, Rabia *et al*. 2016, Kablia *et al*. 2020, Adim *et al*. 2018, Panjehpour *et al*. 2014, Zidour *et al*. 2020, Benferhat *et al*. 2018 and Yang *et al*. 2007) .

One of the classes of composites, the functionally graded material (FGM materials), in this case our objective concerns the study of the of peeling off of the composite plate, due to the high interfacial stress concentrations in a damaged reinforced concrete beams reinforced in bending by imperfect FGM plate. In recent years, several research studies have been carried out on the rehabilitation method (Abualnour *et al*. 2018, Belkacem *et al*. 2016b, Benferhat, *et al*. 2016a, Adim *et al*. 2016, Benhenni *et al*. 2019, Bensattalah *et al*. 2020, Hassaine Daouadji 2013, Benyoucef *et al*. 2007, Rabia *et al*. 2020, Tahar, *et al*. 2016, Tayeb *et al*. 2020, Tlidji *et al*. 2021,Bekki *et al*. 2019, Benferhat *et al*. 2019, El Mahi *et al*. 2014, Hassaine Daouadji *et al*. 2016a, Mohammadimehr *et al*. 2017, Panjehpour *et al*. 2016, Yeghnem *et al*. 2019, Ait Atmane *et al*. 2015, Amara *et al*. 2019, Rabahi *et al*. 2016, Tounsi *et al*. 2008, Mohammadimehr *et al*. 2018, Guenaneche *et al*. 2014 and Krour *et al*. 2014). In this context, we have shown the influence of the different parameters influencing the evolution of the porous FGM / concrete interface stresses of a RC beam such as the effect of the damage concrete, the effect of air bubbles in concrete, the effect of porosity in FGM plate and the influence of prestressing. An improved method for calculating interface stresses has been developed. The validation of the present model was carried out by comparison with those of the most recent results from the literature. Finally, some concluding remarks are summarized in conclusion. It is believed that the present results will be of interest to civil and structural engineers and researchers.

2. Theoretical analysis and solutions procedure:

2.1 Assumptions of the present solution

The present analysis takes into consideration the transverse shear stress and strain in the beam and the plate but ignores the transverse normal stress in them. One of the analytical approach proposed by Benferhat (2018) for damaged reinforced concrete beam strengthened with a bonded imperfect FGM Plate (Fig. 1) was used in order to compare it with another analytical models.

The analytical approach (Hassaine Daouadji *et al*. 2016a and Benferhat *et al*. 2016b) is based on the following assumptions:

- Elastic stress strain relationship for FGM and adhesive;
- There is a perfect bond between the imperfect FGM plate and the beam;
- The adhesive is assumed to only play a role in transferring the stresses from the FGM beam to the composite plate reinforcement;
- The stresses in the adhesive layer do not change through the direction of the thickness

Since the functionally graded materials is an orthotropic material. In analytical study (Belkacem *et al*. 2016a, Benferhat *et al*. 2018, Hassaine Daouadji *et al*. 2008 and Rabahi *et al*. 2019), the classical plate theory is used to determine the stress and strain behaviors of the externally bonded imperfect FGM plate in order to investigate the whole mechanical performance of the composite - strengthened structure.

2.2. Material properties of damaged concrete beams

The model's Mazars is based on elasticity coupled with isotropic damage and ignores any manifestation of plasticity, as well as the closing of cracks (Mazars *et al*. 1996). This concept directly describes the loss of rigidity and the softening behavior. The constraint is determined by the following expression:

$$\sigma_{ij} = (1-d)E_{ij}\varepsilon_{ij} \qquad 0 < d < 1 \tag{1}$$

$$\tilde{E}_{11} = E_{11}(1-d) \text{ long} \tag{2}$$

$$\tilde{E}_{22} = E_{22}(1-d) \text{ trans} \tag{3}$$

where $\tilde{E}_{11}$, $\tilde{E}_{22}$ and E_{11}, E_{22} are the elastic constants of damaged and undamaged state, respectively. "d" is damaged variable. Hence, the material properties of the damaged beam can be represented by replacing the above elastic constants with the effective ones defined in Eqs. (2) and (3).

2.3. Distribution forms of the air bubbles in the concrete beam:

Because of manufacturing defects in concrete such as the air bubbles "α" that are the subject of the subject, the Young's modulus (E_1) of the imperfect reinforced concrete beam can be written as a functions of thickness coordinate. Several forms of porosity (air bubbles in concrete) have been studied in the present work, which is written in the following forms:

$$E_1 = E_b(1-\alpha) \tag{4}$$

$$\sigma_{ij} = (1-\alpha)E_{ij}\varepsilon_{ij} \tag{5}$$

where E_b is the elastic constants of concrete and α is the index of air bubbles in concrete.

2.4. Properties of the FGM constituent materials

In this study, we consider an imperfect FGM plate with a volume fraction of porosity δ(δ<< 1), with different form of distribution between the metal and the ceramic. The modified mixture rule proposed by (Bekki 2019, Hassaine Daouadji 2017, Rabahi *et al*. 2018 and Benferhat 2019) is:

$$P = P_m(V_m - \frac{\delta}{2}) + P_c((\frac{z}{h} + \frac{1}{2})^k - \frac{\delta}{2}) \tag{6}$$

The modified mixture rule becomes:

$$P = (P_c - P_m)(\frac{z}{h} + \frac{1}{2})^k + P_m - (P_c + P_m)\frac{\delta}{2} \tag{7}$$

Where, k is the power law index that takes values greater than or equals to zero. The FGM plate becomes a fully ceramic plate when k is set to zero and fully metal for large value of k. The Young's modulus (E) of the imperfect FG plate can be written as a functions of thickness coordinate, z (middle surface). The material properties of a perfect FGM plate can be obtained when the volume fraction of porosity α is set to zero. Due to the small variations of the Poisson ratio ν, it is assumed to be constant. Several forms of porosity have been studied in the present work, such as uniform distribution "O", "X", "V" and Inverted "V" as follows (Benferhat *et al*. 2020, Bekki *et al*. 2019, Adim *et al*. 2016 and Hassaine Daouadji *et al*. 2019), including the deferent's distribution forms of porosity which come in the forms below:

Uniform distribution shape of the porosity

$$E_2(z) = (e_c - e_m) * ((\frac{z}{t_2} + 0.5))^k + e_m - (e_c + e_m) * \frac{\delta}{2} \tag{8}$$

Form "X" distribution shape of the porosity

$$E_2(z) = (e_c - e_m) * ((\frac{z}{t_2} + 0.5))^k + e_m - (e_c + e_m) * \frac{\delta}{2} * (2 * \frac{z}{t_2}) \tag{9}$$

Form "O" distribution shape of the porosity

$$E_2(z) = (e_c - e_m) * ((\frac{z}{t_2} + 0.5))^k + e_m - (e_c + e_m) * \frac{\delta}{2} * (1 - 2 * \frac{|z|}{t_2}) \tag{10}$$

Form "V" distribution shape of the porosity

$$E_2(z) = (e_c - e_m) * ((\frac{z}{t_2} + 0.5))^k + e_m - (e_c + e_m) * \frac{\delta}{2} * (\frac{1}{2} + \frac{z}{t_2}) \tag{11}$$

Inverted Form "V" distribution shape of the porosity

$$E_2(z) = (e_c - e_m) * ((\frac{z}{t_2} + 0.5))^k + e_m - (e_c + e_m) * \frac{\delta}{2} * (\frac{1}{2} - \frac{z}{t_2}) \tag{12}$$

Being given that $E_2(z)$ is determined according to the form of distribution of the porosity in the imperfect FGM plate, given by the Eqs. (8), (9), (10), (11) and (12), the linear constitutive relations of a FGM plate can be written as:

$$\begin{Bmatrix} \sigma_x \\ \sigma_y \\ \tau_{yz} \\ \tau_{xz} \\ \tau_{xy} \end{Bmatrix} = \begin{bmatrix} \frac{E_2(z)}{1-\nu^2} & \frac{\nu E_2(z)}{1-\nu^2} & 0 & 0 & 0 \\ \frac{\nu E_2(z)}{1-\nu^2} & \frac{E_2(z)}{1-\nu^2} & 0 & 0 & 0 \\ 0 & 0 & \frac{E_2(z)}{2(1+\nu)} & 0 & 0 \\ 0 & 0 & 0 & \frac{E_2(z)}{2(1+\nu)} & 0 \\ 0 & 0 & 0 & 0 & \frac{E_2(z)}{2(1+\nu)} \end{bmatrix} \begin{Bmatrix} \varepsilon_x \\ \varepsilon_y \\ \gamma_{yz} \\ \gamma_{xz} \\ \gamma_{xy} \end{Bmatrix} \tag{13}$$

where (σ_x, σ_y, τ_{xy}, τ_{yz}, τ_{yx}) and (ε_x, ε_y, γ_{xy}, γ_{yz}, γ_{yx}) are the stress and strain components, respectively , and A_{ij}, D_{ij} are the plate stiffness, defined by:

$$A_{ij} = \int_{-h/2}^{h/2} Q_{ij} dz \cdots\cdots D_{ij} = \int_{-h/2}^{h/2} Q_{ij} z^2 dz \tag{14}$$

where A'_{11}, D'_{11} are defined as:

$$A'_{11} = \frac{A_{22}}{A_{11}A_{22} - A_{12}^2} \qquad D'_{11} = \frac{D_{22}}{D_{11}D_{22} - D_{12}^2} \tag{15}$$

3. Mathematical formulation of the present method

3.1. Shear stress distribution along the imperfect FGM concrete interface

The governing differential equation for the interfacial shear stress is expressed as (Hassaine Daouadji 2016a and Rabia *et al*. 2019):

$$\frac{d^2\tau(x)}{dx^2}-\frac{1}{\frac{t_a}{G_a}+\frac{t_1}{4G_1}}\left(A_{11}^{'}+\frac{b_2}{E_1A_1}+\frac{(y_1+t_2/2)(y_1+t_a+t_2/2)}{E_1I_1D_{11}^{'}+b_2}b_2D_{11}^{'}\right)\tau(x)+\frac{1}{\frac{t_a}{G_a}+\frac{t_1}{4G_1}}\left(\frac{(y_1+t_2/2)}{E_1I_1D_{11}^{'}+b_2}D_{11}^{'}\right)V_T(x)=0 \tag{16}$$

For simplicity, the general solutions presented below are limited to loading which is either concentrated or uniformly distributed over part or the whole span of the beam, or both. For such loading, $\frac{d^2V_T(x)}{dx^2}=0$, and the general solution to Eq. (16) is given by:

$$\tau(x)=\eta_1\cosh(\chi_1x)+\eta_2\sinh(\chi_1x)+\chi_2V_T(x) \tag{17}$$

Where

$$\chi_1=\sqrt{\frac{1}{\frac{t_a}{G_a}+\frac{t_1}{4G_1}}\left(A_{11}^{'}+\frac{b_2}{E_1A_1}+\frac{(y_1+t_2/2)(y_1+t_a+t_2/2)}{E_1I_1D_{11}^{'}+b_2}b_2D_{11}^{'}\right)} \tag{18}$$

$$\chi_2=\frac{1}{(\frac{t_a}{G_a}+\frac{t_1}{4G_1})\chi_1^2}\left(\frac{y_1+\frac{t_2}{2}}{E_1I_1D_{11}^{'}+b_2}D_{11}^{'}\right)V_T(x) \tag{19}$$

And η_1 and η_2 are constant coefficients determined from the boundary conditions. In the present study, a simply supported beam has been investigated which is subjected to a uniformly distributed load (Fig. 1). The interfacial shear stress for this uniformly distributed load at any point is written as (Hassaine Daouadji 2016a and Rabia *et al*. 2019), by substituting χ_1 and χ_2 by their expressions cited in Eqs. (18) and (22):

$$\tau(x)=\left[\frac{\frac{K_1y_1}{E_1I_1}a}{2}(L-a)-\frac{1}{(\frac{t_a}{G_a}+\frac{t_1}{4G_1})\xi^2}\left(\frac{y_1+\frac{t_2}{2}}{E_1I_1D_{11}^{'}+b_2}D_{11}^{'}\right)\right]\frac{qe^{-\xi x}}{\xi}+\frac{1}{(\frac{t_a}{G_a}+\frac{t_1}{4G_1})\xi^2}\left(\frac{y_1+\frac{t_2}{2}}{E_1I_1D_{11}^{'}+b_2}D_{11}^{'}\right)q\left(\frac{L}{2}-a-x\right) \qquad 0\le x\le L_P \tag{20}$$

Where q is the uniformly distributed load and x; a; L and L_p are defined in Fig. 1.

3.2. Normal stress distribution along the imperfect FGM concrete interface

The following governing differential equation for the interfacial normal stress (Hassaine Daouadji 2016a and Rabia *et al*. 2019):

$$\frac{d^4\sigma_n(x)}{dx^4}+K_n\left(D_{11}^{'}+\frac{b_2}{E_1I_1}\right)\sigma_n(x)-K_n\left(D_{11}^{'}\frac{t_2}{2}-\frac{y_1b_2}{E_1I_1}\right)\frac{d\tau(x)}{dx}+\frac{qK_n}{E_1I_1}=0 \tag{21}$$

The general solution to this fourth–order differential equation is

$$\sigma_n(x) = e^{-\chi_3 x}\left[\eta_3 \cos(\chi_3 x) + \eta_4 \sin(\chi_3 x)\right] + e^{\chi_3 x}\left[\eta_5 \cos(\chi_3 x) + \eta_6 \sin(\chi_3 x)\right] - \left(\frac{y_1 b_2 - \frac{D'_{11} E_1 I_1 t_2}{2}}{D'_{11} E_1 I_1 + b_2}\right)\frac{d\tau(x)}{dx} - \frac{1}{D'_{11} E_1 I_1 + b_2} q \tag{22}$$

For large values of x it is assumed that the normal stress approaches zero and, as a result, $\eta_5=\eta_6=0$. The general solution therefore becomes

$$\sigma_n(x) = e^{-\chi_3 x}\left[\eta_3 \cos(\chi_3 x) + \eta_4 \sin(\chi_3 x)\right] - \left(\frac{y_1 b_2 - \frac{D'_{11} E_1 I_1 t_2}{2}}{D'_{11} E_1 I_1 + b_2}\right)\frac{d\tau(x)}{dx} - \frac{1}{D'_{11} E_1 I_1 + b_2} q \tag{23}$$

Where

$$\chi_3 = \sqrt[4]{\frac{K_n}{4}\left(D'_{11} + \frac{b_2}{E_1 I_1}\right)} \tag{24}$$

As is described by Hassaine Daouadji (2016a), the constants η_3 and η_4 in Eq. (22) are determined using the appropriate boundary conditions and they are written as follows:

$$\eta_3 = \frac{K_n\left[V_T(0) + \sqrt[4]{\frac{K_n}{4}(D'_{11} + \frac{b_2}{E_1 I_1})} M_T(0)\right]}{2\left[\sqrt[4]{\frac{K_n}{4}(D'_{11} + \frac{b_2}{E_1 I_1})}\right]^3 E_1 I_1} - \frac{b_2 K_n\left(\frac{y_1}{E_1 I_1} - \frac{D'_{11} t_2}{2 b_2}\right)}{2\left[\sqrt[4]{\frac{K_n}{4}(D'_{11} + \frac{b_2}{E_1 I_1})}\right]^3}\tau(0) + \frac{\left[\frac{d^4\tau(0)}{dx^4} + \sqrt[4]{\frac{K_n}{4}(D'_{11} + \frac{b_2}{E_1 I_1})}\frac{d^3\tau(0)}{dx^3}\right]}{2\left[\sqrt[4]{\frac{K_n}{4}(D'_{11} + \frac{b_2}{E_1 I_1})}\right]^3} \tag{25}$$

$$\eta_4 = -\frac{K_n}{2\sqrt{\frac{K_n}{4}(D'_{11} + \frac{b_2}{E_1 I_1}).E_1 I_1}} M_T(0) - \frac{\frac{y_1 b_2 - \frac{D'_{11} E_1 I_1 t_2}{2}}{D'_{11} E_1 I_1 + b_2}}{2\sqrt{\frac{K_n}{4}(D'_{11} + \frac{b_2}{E_1 I_1})}}\frac{d^3\tau(0)}{dx^3} \tag{26}$$

The above expressions for the constants η_3 and η_4 has been left in terms of the bending moment $M_T(0)$ and shear force $V_T(0)$ at the end of the soffit plate. With the constants η_3 and η_4 determined, the interfacial normal stress can then be found using Eq.(21).

4. Results: discussion and analysis

4.1 Material used:

The material used for the present studies is an RC beam bonded with imperfect FGM plate. The beam is simply supported and subjected to a uniformly distributed load. A summary of the geometric and material properties is given in Table 1.

4.2 Comparison of analytical solution:

The present simple solution is compared, in this section, with some approximate solutions available in the literature. These include Rabahi (2016), Benyoucef (2007), Tounsi (2006) and

Table1 Geometric and mechanical properties of the materials used

Materials	E (GPa)	Width (mm)	Thickness (mm)
Ceramic	380	b_2=200	t_2=4 mm
FGM	/	b_2=200	t_2=4 mm
Metal	70	b_2=200	t_2=4 mm
CFRP plate	100	b_2=200	t_2=4 mm
Adhesive	3	b_a=200	t_a=2 mm
RC Beam	30	b_1=200	t_1=300 mm

Table 2 Comparison of the interfacial stresses for the different parameters influencing in an RC beam reinforced by imperfect FGM under uniform distributed load

Theory	Damage variable "*d*"	Porosity index in the FGM "δ"	% of air bubble "α"	τ(x) MPa	σ(x) MPa
Rabahi (2016) - CFRP plate - P=0 kN	0	0	0	1,99822	1,18868
Benyoucef (2007) -CFRP plate- P=0 kN	0	0	0	1,86439	1,11520
Tounsi (2006) - CFRP plate- P=0 kN	0	0	0	1,79155	1,07803
Hassaine Daouadji (2016b) FGM- k=10 plate - P=0 kN	0	0	0	1.6635	1.0064
Present model - FGM plate	0,1	0	0	1,55820	1,08048
	0	0	0	1,46475	1,01194
FGM - k=10 P=0 kN	0	0,1	0	1,24182	0,92526
	0	0,1	0,02	1,25709	0,93733
	0,1	0,1	0,02	1,33883	1,00208

Hassaine Daouadji (2016b) solutions uniformly distributed loads. A comparison of the interfacial shear and normal stresses from the different existing closed – form solutions and the present solution is undertaken in this section. An undamaged beams bonded with CFRP and FGM plate soffit plate is considered. The beam is simply supported and subjected to a uniformly distributed load. A summary of the geometric and material properties is given in table 1. The Table 2 shows the interfacial shear and normal stresses near the plate end for the example beams indicated on Table 2 for the uniformly distributed load case. Overall, the predictions of the different solutions agree closely with each other.

The present analysis gives lower maximum interfacial shear and normal stresses than those predicted by Tounsi (2006), Rabahi (2016) and Benyoucef (2007), indicating that the inclusion of adherend shear deformation effect in the beam and soffit plate leads to lower values of τ_{max} and σ_{max}. However, the maximum interfacial shear and the normal stresses given by the present method are lower than the results from the literature (Tounsi 2006, Rabahi 2016, Benyoucef 2006 and Hassaine Daouadji 2016b). This difference is due to the assumption used in the present theory which is in agreement with the beam theory, and to the choice of the reinforcement material the imperfect FGM compared to the CFRP.

Table 3 Effect of the variation of the damage variable on the interfacial stresses of the RC beam strengthened with a porous FGM plate

Shear Stress P=0, α=0,02; FGM-k=10					
Damage variable	Distribution forms of Porosity				
d	Homogeneous shape δ=0,1	Form "X" Shape δ=0,1	Form "O" Shape δ=0,1	Form "V" Shape δ=0,1	Form Inverted "V" Shape δ=0,1
0	1,257092	1,432673	1,415602	1,333305	1,424218
0,1	1,338829	1,524178	1,506188	1,419365	1,515268
0,2	1,434369	1,630738	1,611716	1,519799	1,621318
0,3	1,548023	1,756909	1,736728	1,639044	1,746917
Shear Stress P=40 kN, α=0,02; FGM-k=10					
0	-3,476256	-2,661839	-2,734716	-3,104023	-2,697786
0,1	-3,182009	-2,381412	-2,453156	-2,816411	-2,416803
0,2	-2,852987	-2,067263	-2,137785	-2,494517	-2,102053
0,3	-2,480644	-1,711087	-1,780267	-2,129891	-1,745218
Normal Stress P=0, α=0,02; GM-k=10					
Damage variable	Distribution forms of Porosity				
d	Homogeneous shape δ=0,1	Form "X Shape δ=0,1	Form "O" Shape δ=0,1	Form "V" Shape δ=0,1	Form Inverted "V" Shape δ=0,1
0	0,9373273	1,006262	0,9997894	0,9679028	1,003063
0,1	1,002084	1,074516	1,067735	1,034265	1,071165
0,2	1,07822	1,154494	1,147377	1,112172	1,150977
0,3	1,169407	1,249882	1,242403	1,205319	1,246187
Normal Stress P=40 kN, α=0,02; FGM-k=10					
0	-2,448095	-1,745215	-1,805364	-2,118518	-1,774815
0,1	-2,239379	-1,555928	-1,614435	-1,918984	-1,584719
0,2	-2,004132	-1,342226	-1,398908	-1,693901	-1,37012
0,3	-1,735497	-1,097781	-1,152407	-1,436656	-1,124663

4.3 Parametric studies:

4.3.1 Effect of the variation of the damage variable on the interfacial stresses

The analysis of the effect of the variation of the damage variable on the interfacial stresses of the RC beam enhanced with a porous FGM plate (Table 3, Figs. 2 and 3), since there are several parameters influencing interface stresses (shear stress and normal stress), given that by setting three parameters; namely the index of air bubbles at α=0.02 (%); the degree of homogeneity of the FGM k=10 and the prestressing force at P=0 kN and then at P=40 kN. in order to analyze the effect of the damage (from healthy material d=0; to damaged material d=0,1; d=0,2 and d=0,3) on the distribution forms of porosity in the FGM plate (homogeneous shape, form "X" shape, form "O" shape, form "V" shape and inverted form "V" shape) where the porosity index is fixed at δ=0,1.

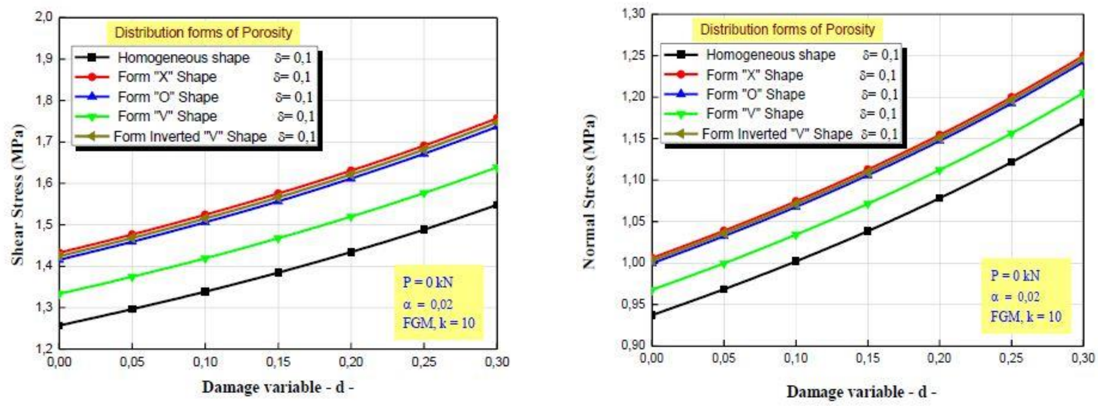

Fig. 2 Effect of the variation of the damage variable on the interfacial stresses of the RC beam strengthened with a porous FGM plate for P=0 kN

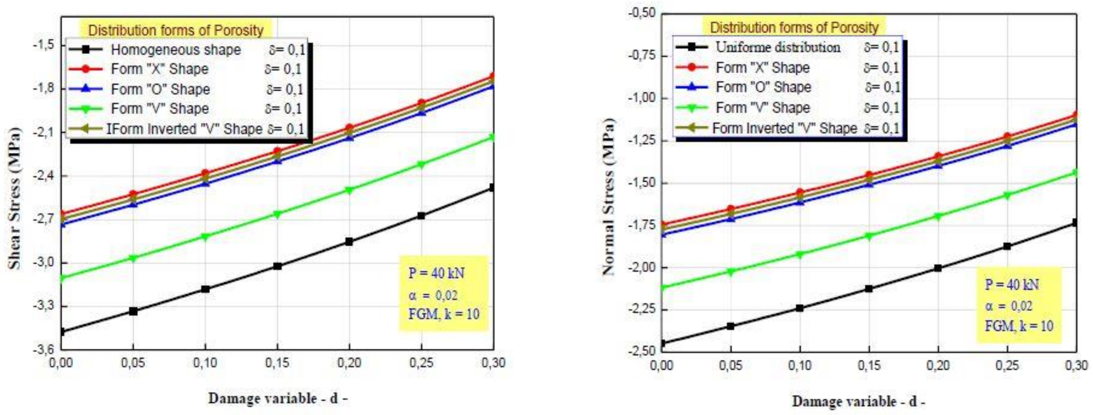

Fig. 3 Effect of the variation of the damage variable on the interfacial stresses of the RC beam strengthened with a porous FGM plate for P=40 kN

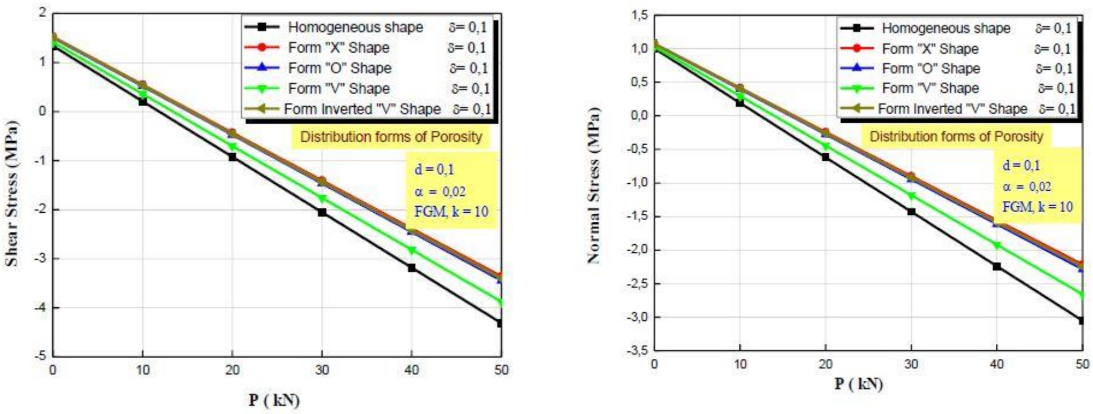

Fig. 4 Effect of prestressing force on the interfacial stresses of the RC beam strengthened with a porous FGM plate

Table 4 Effect of prestressing force on the interfacial stresses of the RC beam strengthened with a porous FGM plate

Prestressing force	Distribution forms of Porosity				
	Shear Stress d=0,1; α=0,02; FGM-k=10				
P (kN)	Homogeneous shape δ=0,1	Form "X" Shape δ=0,1	Form "O" Shape δ=0,1	Form "V" Shape δ=0,1	Form Inverted "V" Shape δ=0,1
0	1,338828	1,524178	1,506187	1,419364	1,515267
10	0,208619	0,547781	0,5163514	0,360421	0,5322498
30	-2,051799	-1,405013	-1,46332	-1,757465	-1,433785
50	-4,312217	-3,357807	-3,442991	-3,875351	-3,399819
	Normal Stress d=0,1; α=0,02; FGM-k=10				
0	1,002084	1,074516	1,067734	1,034263	1,071164
10	0,1917188	0,4169054	0,397192	0,2959528	0,4071934
30	-1,429011	-0,8983158	-0,9438916	-1,180668	-0,9207478
50	-3,049742	-2,213537	-2,284977	-2,657288	-2,248689

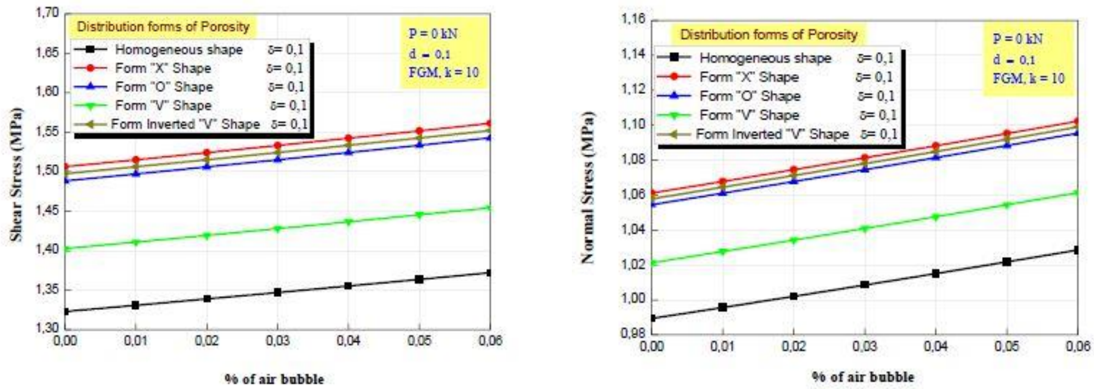

Fig. 5 Effect of air bubble percentage on the interfacial stresses of the RC beam strengthened with a porous FGM plate for P=0 kN

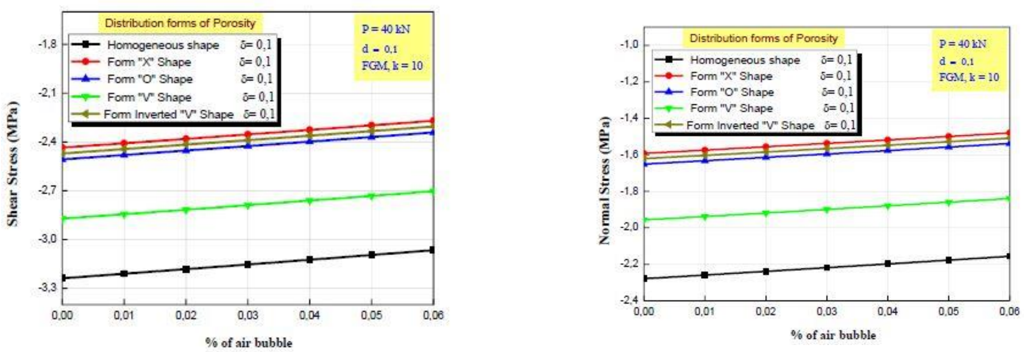

Fig. 6 Effect of air bubble percentage on the interfacial stresses of the RC beam strengthened with a porous FGM plate for P=40 kN

Table 5 Effect of air bubble percentage on the interfacial stresses of the RC beam strengthened with a porous FGM plate

Shear Stress P=0, d=0,1; FGM-k=10					
% of air bubble	Distribution forms of Porosity				
α	Homogeneous shape δ=0,1	Form "X" Shape δ=0,1	Form "O" Shape δ=0,1	Form "V" Shape δ=0,1	Form Inverted "V" Shape δ=0,1
0	1,322885	1,506352	1,488538	1,402587	1,497529
0,02	1,338829	1,524178	1,506188	1,419365	1,515268
0,04	1,355237	1,542509	1,524338	1,436626	1,53351
0,06	1,372128	1,561368	1,543013	1,45439	1,552277
Shear Stress P=40 kN, d=0,1; FGM-k=10					
0	-3,23845	-2,435242	-2,507202	-2,871601	-2,470739
0,02	-3,182009	-2,381412	-2,453156	-2,816411	-2,416803
0,04	-3,124397	-2,326447	-2,397976	-2,76007	-2,361733
0,06	-3,065575	-2,270309	-2,341616	-2,702535	-2,305486
Normal Stress P=0, d=0,1; FGM-k=10					
% of air bubble	Distribution forms of Porosity				
α	Homogeneous shape δ=0,1	Form "X" Shape δ=0,1	Form "O" Shape δ=0,1	Form "V" Shape δ=0,1	Form Inverted "V" Shape δ=0,1
0	0,9894252	1,061191	1,054466	1,021297	1,057866
0,02	1,002084	1,074516	1,067735	1,034265	1,071165
0,04	1,015126	1,088239	1,081394	1,047618	1,084854
0,06	1,028566	1,102369	1,095465	1,061377	1,098958
Normal Stress P=40 kN, d=0,1; FGM-k=10					
0	-2,279536	-1,592369	-1,651192	-1,957387	-1,621317
0,02	-2,239379	-1,555928	-1,614435	-1,918984	-1,584719
0,04	-2,198329	-1,518663	-1,576854	-1,879721	-1,547301
0,06	-2,156356	-1,48055	-1,538411	-1,83957	-1,509025

We noted that more the variable of damage increases more the interface stresses become important in other words that more the rigidity of the RC beam decreases more we recorded more important stresses where the peeling off of the strengthening imperfect FGM plate approaches, also the best distribution forms of porosity which registers a low constraint is the homogeneous shape, object of our research since we aim to decrease these values of the stresses; to ensure proper strengthening of the plate.

The results presented on Table 4 and Fig. 4, on the effect of prestressing force on the interfacial stresses of the RC beam strengthened with a porous FGM plate, keeping the three parameters fixed; namely the index of air bubbles at α=0,02 (%); the degree of homogeneity of the FGM k=10 and the damage variable d=0,1. To show the aforementioned we varied the prestressing force to 0 and then to 50 kN; it is just to see the influence of this force on the interfacial stresses; and the distribution forms of porosity in the FGM plate (homogeneous shape, form “X” shape, form “O” shape, form “V” shape and inverted form “V” shape) where the porosity index is fixed at δ=0,1. In the light of these results we can say that the more the tension plate is tightened (force P increases) the lower the values of the stresses will be; therefore the reinforcement becomes stable and the proposed solution will be effective and promising.

4.3.3 Effect of air bubble percentage on the interfacial stresses

The study of the effect of air bubble percentage on the interfacial stresses of the RC beam enhanced with a porous FGM plate (Table 5, Figs. 5 and 6), the same analysis technique is applied, once the degree of homogeneity is fixed of the FGM k=10, the foreclosure P=0 then at P=40 kN and the damage variable d=0,1.

This time we varied the index of air bubbles from α=0 to α=0,06; in parallel the distribution form of porosity in the FGM plate is also tested (homogeneous shape, form “X” shape, “O” shape, form “V” shape and inverted form “V” shape) where the porosity index is fixed at δ=0,1. The calculated results show that the more the fabrication of a perfect concrete (α=0) the more rigid it is and consequently the beam supports well the imposed loading, the lower the values of the stresses therefore we indicate here the reliability of the proposed technique.

5. Conclusions

The interfacial stresses in the imperfect FGM – damaged RC hybrid beam and subjected to a uniformly distributed bending load, were investigated by a present method, taking into account the influence of parameters on interfacial stresses such as the index of air bubbles of concrete; the degree of homogeneity of the imperfect FGM, the damage variable, the distribution forms of porosity and prestressing force. The adherend shear deformations have been included in the theoretical analyses by assuming linear shear stress distributions through the thickness of the adherends. The results show that the damage and air bubbles of concrete has a significant effect on the interfacial stresses in imperfect FGM -damaged RC beam, similarly for the porosity index of the reinforcement plate. Unlike to the classical solutions, the present solution is general in nature and may be applicable to all kinds of materials.

Acknowledgments

This research was supported by the Algerian Ministry of Higher Education and Scientific Research (MESRS) as part of the grant for the PRFU research project n° A01L02UN140120200002 and by the University of Tiaret, in Algeria.

References

Abdelhak, Z., Hadji, L., Daouadji, T.H. and Adda Bedia, E.A. (2016), “Thermal buckling response of functionally graded sandwich plates with clamped boundary conditions”, *Smart Struct. Syst.*, **18**(2), 267-

291. https://doi.org/10.12989/sss.2016.18.2.267

Abderezak, R., Daouadji, T.H. and Rabia, B. (2020), "Analysis of interfacial stresses of the reinforced concrete foundation beams repairing with composite materials plate", *Coupled Syst. Mech.*, **9**(5), 473-498. http://dx.doi.org/10.12989/csm.2020.9.5.473.

Abderezak, R., Daouadji, T.H., Abbes, B., Rabia, B., Belkacem, A. and Abbes, F. (2018), "Elastic analysis of interfacial stress concentrations in CFRP-RC hybrid beams: Effect of creep and shrinkage", Advan. Mater. Res., **6**(3), 257-278. https://doi.org/10.12989/amr.2017.6.3.257.

Abderezak, R., Daouadji, T.H., Rabia, B. and Belkacem, A. (2018), "Nonlinear analysis of damaged RC beams strengthened with glass fiber reinforced polymer plate under symmetric loads", *Earthq. Struct.*, **15**(2), 113-122. https://doi.org/10.12989/eas.2018.15.2.113.

Abderezak, R., Rabia, B., Daouadji, T.H., Abbes, B., Belkacem, A. and Abbes, F. (2019), "Elastic analysis of interfacial stresses in prestressed PFGM-RC hybrid beams", *Advan. Mater. Res.*, **7**(2), 83-103. https://doi.org/10.12989/amr.2018.7.2.083.

Abualnour, M., Houari, M.S.A., Tounsi, A. and Mahmoud, S.R. (2018), "A novel quasi-3D trigonometric plate theory for free vibration analysis of advanced composite plates", *Compos. Struct.*, **184**, 688-697. https://doi.org/10.1016/j.compstruct.2017.10.047.

Adim, B. and Daouadji, T.H. (2016), "Effects of thickness stretching in FGM plates using a quasi-3D higher order shear deformation theory", *Advan. Mater. Res.*, **5**(4), 223-244. https://doi.org/10.12989/amr.2016.5.4.223.

Adim, B., Daouadji, T.H. and Abbes, B. (2016a), "Buckling analysis of anti-symmetric cross-ply laminated composite plates under different boundary conditions", *Int. Appl. Mech.*, **52**(6), 126-141. https://doi.org/10.1007/s10778-016-0787-x.

Adim, B., Daouadji, T.H. and Abbes, B. (2016b), "Buckling and free vibration analysis of laminated composite plates using an efficient and simple higher order shear deformation theory", *Mech. Ind.*, **17**, 512. https://doi.org/10.1051/meca/2015112.

Adim, B., Daouadji, T.H., Rabia, B. and Hadji, L. (2016), "An efficient and simple higher order shear deformation theory for bending analysis of composite plates under various boundary conditions", *Earthq. Struct.*, **11**(1), 63-82. https://doi.org/10.12989/eas.2016.11.1.063.

Ait Atmane, H., Tounsi, A. and Bernard, F. (2015), "Effect of thickness stretching and porosity on mechanical response of a functionally graded beams resting on elastic foundations", *Int. J. Mech. Mater. Des.*, **13**(1), 71-84. https://doi.org/10.1007/s10999-015-9318-x.

Amara K., Antar, K. and Samir B. (2019), "Hygrothermal effects on the behavior of reinforced-concrete beams strengthened by bonded composite laminate plates", *Struct. Eng. Mech.*, **69**(3), 327-334. https://doi.org/10.12989/sem.2019.69.3.327.

Belkacem, A., Tahar, H.D., Abderrezak, R., Amine, B.M., Mohamed, Z. and Boussad, A. (2018), "Mechanical buckling analysis of hybrid laminated composite plates under different boundary conditions", *Struct. Eng. Mech.*, **66**(6), 761-769. https://doi.org/10.12989/sem.2018.66.6.761.

Benferhat, R., Daouadji, T.H. and Adim, B. (2016b), "A novel higher order shear deformation theory based on the neutral surface concept of FGM plate under transverse load", *Advan. Mater. Res.*, **5**(2), 107-120. https://doi.org/10.12989/amr.2016.5.2.107.

Benferhat, R., Daouadji, T.H. and Mansour, M.S. (2016), "Free vibration analysis of FG plates resting on the elastic foundation and based on the neutral surface concept using higher order shear deformation theory", *Comptes Rendus Mecanique*, **344**(9), 631-641. https://doi.org/10.1016/j.crme.2016.03.002.

Benferhat, R., Hassaine Daouadji, T., Said Mansour, M. and Hadji L. (2016a), "Effect of porosity on the bending and free vibration response of functionally graded plates resting on Winkler-Pasternak foundations", *Earthq. Struct.*, **10**(6), 1429-1449. https://doi.org/10.12989/eas.2016.10.6.1429.

Benhenni, M.A., Daouadji, T.H., Abbes, B., Abbes, F., Li, Y. and Adim, B. (2019), "Numerical analysis for free vibration of hybrid laminated composite plates for different boundary conditions", Struct. Eng. Mech. **70**(5), 535-549. https://doi.org/10.12989/sem.2019.70.5.535.

Benhenni, M.A., Daouadji, T.H., Abbes, B., Adim, B., Li, Y. and Abbes, F. (2018)., "Dynamic analysis for anti-symmetric cross-ply and angle-ply laminates for simply supported thick hybrid rectangular plates", *Advan. Mater. Res.*, **7**(2), 83-103. https://doi.org/10.12989/amr.2018.7.2.119.

Bensattalah, T., Daouadji, T.H. and Zidour, M. (2020), "Influences the shape of the floor on the behavior of buildings under seismic effect", *Proceedings of the 4th International Symposium on Materials and Sustainable Development*, https://doi.org/10.1007/978-3-030-43268-3_3.

Bensattalah, T., Zidour, M. and Daouadji, T.H. (2018), "Analytical analysis for the forced vibration of CNT surrounding elastic medium including thermal effect using nonlocal Euler-Bernoulli theory" Advan. Mater. Res., **7**(3), 163-174. https://doi.org/10.12989/amr.2018.7.3.163.

Benyoucef, S, Tounsi, A, Meftah, S.A. and Adda Bedia, E.A. (2007), "Approximate analysis of the interfacial stress concentrations in FRP-RC hybrid beams", *Compos. Interfaces*, **13**(7), 561-571. https://doi.org/10.1163/156855406778440758.

Chedad, A., Daouadji, T.H., Abderezak, R., Belkacem, A., Abbes, B., Rabia, B. and Abbes, F. (2018), "A high-order closed-form solution for interfacial stresses in externally sandwich FGM plated RC beams", *Advan. Mater. Res.*, **6**(4), 317-328. https://doi.org/10.12989/amr.2017.6.4.317.

Chergui, S., Daouadji, T.H., Hamrat, M., Boulekbache, B., Bougara, A., Abbes, B. and Amziane, S. (2019), "Interfacial stresses in damaged RC beams strengthened by externally bonded prestressed GFRP laminate plate: Analytical and numerical study", *Advan. Mater. Res.*, **8**(3), 197-217. https://doi.org/10.12989/amr.2019.8.3.197.

Chikr, S.C., Kaci, A., Yeghnem, R. and Tounsi, A. (2019), "A new higher-order shear and normal deformation theory for the buckling analysis of new type of FGM sandwich plates", *Struct. Eng. Mech.* **72**(5), 653-673. https://doi.org/10.12989/sem.2019.72.5.653.

Daouadji, T.H., Chedad, A. and Adim, B. (2016b), "Interfacial stresses in RC beam bonded with a functionally graded material plate", *Struct. Eng. Mech.*, **60**(4), 693-705. http://dx.doi.org/10.12989/sem.2016.60.4.693.

Daouadji, T.H., Rabahi, A., Abbes, B. and Adim, B. (2016a), "Theoretical and finite element studies of interfacial stresses in reinforced concrete beams strengthened by externally FRP laminates plate", *J. Adhesion Sci. Technol.*, 30(12), 1253-1280. https://doi.org/10.1080/01694243.2016.1140703.

Guenaneche, B. and Tounsi, A. (2014), "Effect of shear deformation on interfacial stress analysis in plated beams under arbitrary loading", *Adhesion Adhesives*, **48**, 1-13. https://doi.org/10.1016/j.ijadhadh.2013.09.016.

Hadj, B., Rabia, B. and Daouadji, T.H. (2019), "Influence of the distribution shape of porosity on the bending FGM new plate model resting on elastic foundations", *Struct. Eng. Mech.*, **72**(1), 823-832. https://doi.org/10.12989/sem.2019.72.1.061.

Hadji, L., Daouadji, T.H. and Bedia, E.A. (2015), "A refined exponential shear deformation theory for free vibration of FGM beam with porosities", *Geomech. Eng.*, **9**(3), 361-372. https://doi.org/10.12989/gae.2015.9.3.361.

Hamrat, M., Bouziadi, F., Boulekbache, B., Daouadji, T.H., Chergui, S., Labed, A. and Amziane, S. (2020), "Experimental and numerical investigation on the deflection behavior of pre-cracked and repaired reinforced concrete beams with fiber-reinforced polymer", *Construct. Build. Mater.*, **249**(20), 1-13. http://dx.doi.org/10.1016/j.conbuildmat.2020.118745.

Hassaine Daouadji, T. (2013), "Analytical analysis of the interfacial stress in damaged reinforced concrete beams strengthened by bonded composite plates", *Strength Mater.*, **45**(5), 587-597. https://doi.org/10.1007/s11223-013-9496-4.

Hassaine Daouadji, T. (2017), "Analytical and numerical modeling of interfacial stresses in beams bonded with a thin plate", *Advan. Comput. Des.*, **2**(1), 57-69. https://doi.org/10.12989/acd.2017.2.1.057.

Hassaine Daouadji, T., Benyoucef, S. and Adda B. (2008), "Interfacial stresses concentrations in FRP - damaged RC hybrid beams", *Compos. Interfaces*, **15**, 425-440. https://doi.org/10.1163/156855408784514702.

Hassaine Daouadji, T., Rabahi, A. and Benferhat, R. (2020), "Flexural performance of wooden beams strengthened by composite plate", *Struct. Monit. Maint.*, **7**(3), 233-259. http://dx.doi.org/10.12989/smm.2020.7.3.233.

Kablia, A., Benferhat, R., Hassaine Daouadji, T. and Bouzidene A. (2020), "Effect of porosity distribution rate for bending analysis of imperfect FGM plates resting on Winkler-Pasternak foundations under various boundary conditions", *Coupled Syst. Mech.*, **9**(6), 575-597. http://dx.doi.org/10.12989/csm.2020.9.6.575.

Krour, B., Bernard, F. and Tounsi, A. (2014), "Fibers orientation optimization for concrete beam strengthened with a CFRP bonded plate: A coupled analytical-numerical investigation", *Eng. Struct.*, **9**, 218-227. https://doi.org/10.1016/j.engstruct.2013.05.008

Mahi, B.E., Benrahou, K.H., Belakhdar, K., Tounsi, A. and Bedia, E.A. (2014), "Effect of the tapered of the end of a FRP plate on the interfacial stresses in a strengthened beam used in civil engineering applications", *Mech. Compos. Mater.*, **50**(4), 465-474. https://doi.org/10.1007/s11029-014-9433-z.

Mazars, J. and Pijaudier-Cabot, G. (1996), "From damage to fracture mechanics and conversely: A combined approach", *Int. J. Solids Struct.*, **33**(20), 3327-3342. https://doi.org/10.1016/0020-7683(96)00015-7.

Mohammadimehr, M., Hooyeh, H.M., Afshari, H. and Salarkia, M.R. (2017), "Free vibration analysis of double bonded isotropic piezoelectric Timoshenko micro-beam based on strain gradient and surface stress elasticity theories under initial stress using DQM", *Mech. Advan. Mater. Struct.*, **24**(4), 287-303. https://doi.org/10.1080/15376494.2016.1142022.

Mohammadimehr, M., Mehrabi, M., Hadizadeh, H. and Hadizadeh, H. (2018), "Surf ace and size dependent effects on static, buckling, and vibration of micro composite beam under thermomagnetic fields based on strain gradient theory", *Steel Compos. Struct.*, **26**(4), 513-531. https://doi.org/10.12989/scs.2018.26.4.513.

Panjehpour Mohammad, Abang Abdullah Abang Ali,Yen Lei Voo and Farah Nora Aznieta (2014), "Effective compressive strength of strut in CFRP-strengthened reinforced concrete deep beams following ACI 318-11", *Comput. Concrete*, **13**(1), 135-165 https://doi.org/10.12989/cac.2014.13.1.135.

Panjehpour, M., Farzadnia, N., Demirboga, R. and Ali, A.A.A. (2016), "Behavior of high-strength concrete cylinders repaired with CFRP sheets", *J. Civil Eng. Manage.*, **22**(1), 56-64. https://doi.org/10.3846/13923730.2014.897965.

Rabahi, A., Daouadji, T.H., Abbes, B. and Adim, B. (2016), "Analytical and numerical solution of the interfacial stress in reinforced-concrete beams reinforced with bonded prestressed composite plate", *J. Reinforced Plastics Compos.*, **35**(3) 258-272. https://doi.org/10.1177/0731684415613633.

Rabia, B., Abderezak, R., Daouadji, T.H., Abbes, B., Belkacem, A. and Abbes, F. (2018), "Analytical analysis of the interfacial shear stress in RC beams strengthened with prestressed exponentially-varying properties plate", *Advan. Mater. Res.*, **7**(1), 29-44. https://doi.org/10.12989/amr.2018.7.1.029.

Rabia, B., Daouadji, T.H. and Abderezak, R. (2019), "Effect of distribution shape of the porosity on the interfacial stresses of the FGM beam strengthened with FRP plate", *Earthq. Struct.*, **16**(50), 601-609. https://doi.org/10.12989/eas.2019.16.5.601.

Rabia, B., Daouadji, T.H. and Abderezak, R. (2019), "Effect of porosity in interfacial stress analysis of perfect FGM beams reinforced with a porous functionally graded materials plate", *Struct. Eng. Mech.*, **72**(3), 293-304. https://doi.org/10.12989/sem.2019.72.3.293.

Rabia, B., Hassaine Daouadji, T. and Rabahi, A. (2020), "Predictions of the maximum plate end stresses of imperfect FRP strengthened RC beams: study and analysis", *Advan. Mater. Res.*, **9**(4), 265-287. http://dx.doi.org/10.12989/amr.2020.9.4.265.

Rabia, B., Tahar, H.D. and Abderezak, R. (2020), "Thermo-mechanical behavior of porous FG plate resting on the Winkler-Pasternak foundation", *Coupled Syst. Mech.*, **9**(6), 499-519. http://dx.doi.org/10.12989/csm.2020.9.6.499.

Smith, S.T. and Teng, J.G. (2002), "Interfacial stresses in plated beams", *Eng. Struct.*, **23**(7), 857-871. http://dx.doi.org/10.1016/S0141-0296(00)00090-0.

Tahar, H.D., Boussad, A., Abderezak, R., Rabia, B., Fazilay, A. and Belkacem, A. (2019), "Flexural behaviour of steel beams reinforced by carbon fiber reinforced polymer: Experimental and numerical study", *Struct. Eng. Mech.*, **72**(4), 409-419. https://doi.org/10.12989/sem.2019.72.4.409.

Tahar, H.D., Lazreg, H., Mohamed A.A.M. and Hadj, B. (2016), "Elastic analysis effect of adhesive layer characteristics in steel beam strengthened with a fiber-reinforced polymer plates", *Struct. Eng. Mech.*, **59**(1), 83-100. https://doi.org/10.12989/sem.2016.59.1.083.

Tayeb, B. and Daouadji, T.H. (2020), "Improved analytical solution for slip and interfacial stress in composite steel-concrete beam bonded with an adhesive", *Advan. Mater. Res.*, **9**(2), 133-153. https://doi.org/10.12989/amr.2020.9.2.133.

Tayeb, T.S., Zidour, M., Bensattalah, T., Heireche, H., Benahmed, A. and Bedia, E.A. (2020), "Mechanical buckling of FG-CNTs reinforced composite plate with parabolic distribution using Hamilton's energy principle", *Advan. Nano Res.*, **8**(2), 135-148. https://doi.org/10.12989/anr.2020.8.2.135.

Tlidji, Y., Benferhat, R. and Tahar, H.D. (2021), "Study and analysis of the free vibration for FGM microbeam containing various distribution shape of porosity", *Struct. Eng. Mech.*, **77**(2), 217-229. http://dx.doi.org/10.12989/sem.2021.77.2.217

Tounsi, A. (2006), "Improved theoretical solution for interfacial stresses in concrete beams strengthened with FRP plate", *Int. J. Solids Struct.*, **43**, 14-15, 4154-4174. https://doi.org/10.1016/j.ijsolstr.2005.03.074.

Tounsi, A., Daouadji, T.H. and Benyoucef, S. (2008), "Interfacial stresses in FRP-plated RC beams: Effect of adherend shear deformations", *Int. J. Adhesion Adhesives*, **29**, 313-351. https://doi.org/10.1016/j.ijadhadh.2008.06.008.

Yang, J. and Wu, Y.F. (2007), "Interfacial stresses of FRP strengthened concrete beams: Effect of shear deformation", *Compos. Struct.*, 80(2007), 343-351. https://doi.org/10.1016/j.compstruct.2006.05.016.

TK